

Simple chaotic systems and circuits

J. C. Sprott^{a)}

Department of Physics, University of Wisconsin, Madison, Wisconsin 53706

(Received 25 August 1999; accepted 29 November 1999)

Many new chaotic systems with algebraically simple representations are described. These systems involve a single third-order autonomous ordinary differential equation (jerk equation) with various nonlinearities. Piecewise linear functions are emphasized to permit easy electronic implementation with diodes and operational amplifiers. Several new simple and robust chaotic electrical circuits are described and evaluated. © 2000 American Association of Physics Teachers.

I. INTRODUCTION

In 1963, Lorenz¹ published a seminal paper in which he showed that what we now call chaos can occur in systems of autonomous ordinary differential equations (ODEs) with as few as three variables and two quadratic nonlinearities. In 1976, Rössler² found a similar system, but with a single quadratic nonlinearity. Both the Lorenz and Rössler systems contain seven terms when written as three first-order ODEs. In 1979, Rössler³ found a toroidal chaotic system with six terms and one quadratic nonlinearity. In 1994, Sprott⁴ performed an extensive computer search in which he found fourteen additional chaotic systems with six terms and one quadratic nonlinearity and five systems with five terms and two quadratic nonlinearities. Gottlieb⁵ noted that at least some of these systems could be written as a single third-order ODE and posed the question “What is the simplest jerk function that gives chaos?” By “jerk function,” he means a function J such that the third-order ODE can be written in the form $\ddot{x} = J(\dot{x}, \dot{x}, x)$, where J can be considered the time derivative of an acceleration \dot{x} . In response, Linz⁶ showed that the Lorenz and the original Rössler models have rather complicated functional forms for J , but that Sprott’s model R can be written as

$$\ddot{x} = -\dot{x} - 0.9x + x\dot{x} - 0.4. \quad (1)$$

Meanwhile, Sprott⁷ found several other simple functions J that lead to chaos with a single quadratic or cubic nonlinearity, including one⁸ with only three terms:

$$\ddot{x} = -2.017\dot{x} + \dot{x}^2 - x. \quad (2)$$

Eichhorn *et al.*⁹ further showed that all fourteen of Sprott’s original models with six terms and one quadratic nonlinearity as well as Eq. (2) and Rössler’s toroidal model can be grouped into seven classes of polynomial functions with increasing complexity. Fu and Heidel^{10,11} showed that quadratic functions with fewer than three terms cannot be chaotic, and so Eq. (2) with its variants appears to be the simplest quadratic jerk function that exhibits chaos.

To make further progress, we consider systems of the form:

$$\ddot{x} = a_1\dot{x} + a_2\varphi(\dot{x}) + a_3\dot{x} + a_4\varphi(\dot{x}) + a_5x + a_6\varphi(x) + a_7, \quad (3)$$

where $\varphi(x)$ is a simple nonlinear function chosen to permit electronic implementation with diodes and operational amplifiers, some examples of which are shown in Fig. 1. The procedure was to specify a form for the nonlinearity, randomly choose three or four of the coefficients a_1 – a_7 to be nonzero with random values including at least one nonlinear-

ity, and choose random initial conditions in the range $(-1.5, 1.5)$. The equations were iterated for 32 000 time steps using a fourth-order Runge–Kutta algorithm with a step size of $\Delta t = 0.05$, while calculating the Lyapunov exponent.¹² A difficulty is that the coefficients can range from minus to plus infinity, but most of the chaotic solutions occur when the coefficients are of order unity. Consequently, the coefficient values were chosen using the function $\tan(\pi r/2)$, where r is a random number uniform in the interval $(-1, 1)$. Note that two of the coefficients can generally be set to ± 1 by renormalizing the variables x and t . The remaining coefficients were arbitrarily put into the leading terms for most cases. Unbounded solutions were eliminated by requiring that $|\dot{x}|$, $|\ddot{x}|$, and $|x|$ never exceed 10, a voltage that will typically saturate an operational amplifier. After several days of computing, those cases with Lyapunov exponents greater than 0.001 (base- e) were examined with a smaller step size ($\Delta t = 0.01$) for at least 10^8 iterations to ensure that the chaos is not a numerical artifact or transient. The program was tested with $\varphi(x) = x^2$ to verify that Eq. (2) emerged. In the process, other simple quadratic functions with chaotic solutions were identified and listed in Table I. Many additional cases with multiple nonlinearities, functional redundancy, or additional terms were found but are omitted from Table I.

Note that the cases in Table I can be grouped into dissipative and conservative systems depending on whether the Lyapunov exponents sum to zero. The sum of the Lyapunov exponents is the rate of volume expansion averaged along the orbit and, for systems such as these, is given simply by $\lambda_1 + \lambda_2 + \lambda_3 = \langle d\ddot{x}/d\dot{x} \rangle = a_1 + a_2 \langle d\varphi(\dot{x})/d\dot{x} \rangle$. If the system is chaotic, the largest Lyapunov exponent λ_1 must be positive, λ_2 must be zero, and λ_3 must be negative. Hence a calculation of λ_1 and $\langle d\ddot{x}/d\dot{x} \rangle$ suffices to determine all the Lyapunov exponents. Dissipative systems have a strange attractor with dimension between two and three, while conservative systems fill a three-dimensional volume. In either case, the initial conditions must be chosen appropriately to ensure that they are in the basin of attraction for the dissipative systems and in the stochastic sea for the conservative systems. Although conservative systems are included in Table I, the interest here is primarily in dissipative systems since they lead to more robust electrical circuits. Avoiding dissipation in an electrical circuit is equivalent to constructing a frictionless mechanical system.

II. ABSOLUTE VALUE CASES

One simple nonlinearity is $\varphi(x) = |x|$. It can be considered a piecewise linear approximation to $\varphi(x) = x^2$ with the non-

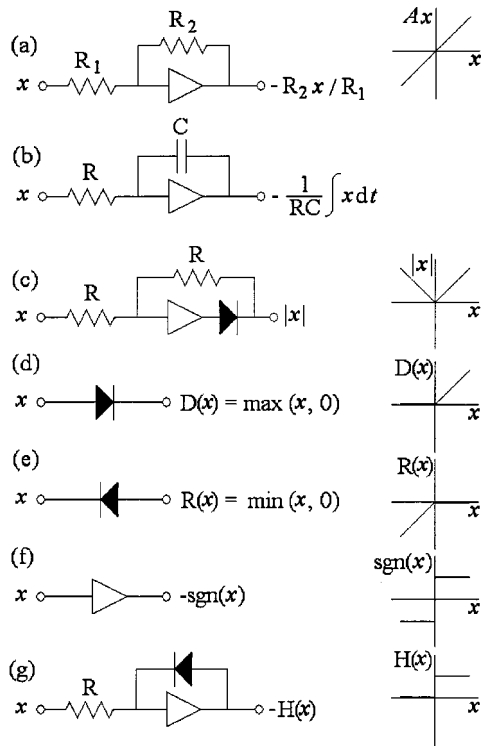


Fig. 1. Some mathematical operations that can be performed with operational amplifiers and ideal diodes. In each case the inverting (−) input to the op amp is used, and the noninverting (+) input is grounded.

linearity confined to the point $x=0$. It has been implemented electronically with a full-wave rectifier with two diodes and an inverting unity-gain amplifier and also with a single diode as shown in Fig. 1(c). Although $d\varphi/dx$ is discontinuous, the

Table I. Some simple chaotic third-order ODE systems and their Lyapunov exponents.

System	Initial conditions (x, \dot{x}, \ddot{x})	Lyapunov exponents (base e)
$\ddot{x} = -2.017 \ddot{x} \pm \dot{x}^2 - x$	(0, 0, ± 1)	0.055, 0, -2.072
$\ddot{x} = -2.8 \ddot{x} \pm x + x^2$	($\mp 0.5, -1, 1$)	0.002, 0, -0.002
$\ddot{x} = -0.44 \ddot{x} - 2\dot{x} \pm (x^2 - 1)$	(0, 0, 0)	0.105, 0, -0.545
$\ddot{x} = -0.5 \ddot{x} - \dot{x} \pm x \pm x^2$	(0, ± 1 , 0)	0.094, 0, -0.594
$\ddot{x} = -2 \ddot{x} \pm (x - 1)$	$\pm(-1, -1, 1)$	0.003, 0, -0.003
$\ddot{x} = -0.6 \ddot{x} - \dot{x} \pm (x - 1)$	(0, 0, 0)	0.036, 0, -0.636
$\ddot{x} = -0.3 \ddot{x} - 0.3 \dot{x} - D(x) + 1$	(0, 0, 0)	0.042, 0, -0.342
$\ddot{x} = -0.3 \ddot{x} - 0.3 \dot{x} - R(x) - 1$	(0, 0, 0)	0.042, 0, -0.342
$\ddot{x} = -2.9 \ddot{x} \pm (0.7x - D(x) + 1)$	$\pm(0, -0.5, 0.5)$	0.003, 0, -0.003
$\ddot{x} = -2.9 \ddot{x} \pm (0.7x - R(x) - 1)$	$\pm(0, 0.5, -0.5)$	0.003, 0, -0.003
$\ddot{x} = -0.5 \ddot{x} - \dot{x} - x + \text{sgn}(x)$	(0, 1, 0)	0.152, 0, -0.652
$\ddot{x} = -0.5 \ddot{x} - \dot{x} + x - \text{sgn}(x)$	(0, 1, 0)	0.601, 0, -1.101
$\ddot{x} = -0.7 \ddot{x} - \dot{x} - x + H(x)$	(0, 1, 0)	0.085, 0, -0.785
$\ddot{x} = -0.4 \ddot{x} - \dot{x} - x + 2S(x)$	(0, 1, 0)	0.072, 0, -0.472
$\ddot{x} = -0.4 \ddot{x} - \dot{x} + x - 2S(x)$	(0, 1, 0)	0.091, 0, -0.491
$\ddot{x} = -0.19 \ddot{x} - \dot{x} - x + 2 \tanh(x)$	(0, 1, 0)	0.128, 0, -0.318
$\ddot{x} = -0.19 \ddot{x} - \dot{x} + x - 2 \tanh(x)$	(0, 1, 0)	0.067, 0, -0.257
$\ddot{x} = -3.7 \ddot{x} \pm (x - x^3)$	(0, $\pm 0.5, 1$)	0.002, 0, -0.002
$\ddot{x} = -0.6 \ddot{x} + 2.8 \dot{x} - \dot{x}^3 - x$	(0, 1, 0)	0.034, 0, -0.634
$\ddot{x} = -0.7 \ddot{x} - \dot{x} + x - x^3$	(0, 1, 0)	0.138, 0, -0.838
$\ddot{x} = -0.35 \ddot{x} - \dot{x} - x + x^3$	(0, 1, 0)	0.082, 0, -0.432
$\ddot{x} = -0.2 \ddot{x} - \dot{x} \pm \sin(x)$	(0, 1, 0)	0.123, 0, -0.323

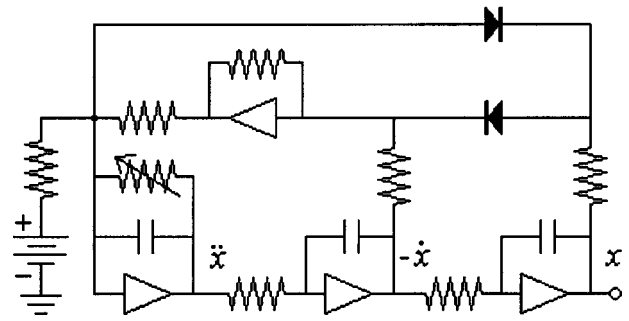


Fig. 2. Chaotic circuit implementation of Eq. (5) using inverting op amps. The diodes are germanium, the battery is 1 V, the capacitors are $0.1 \mu\text{F}$, and the resistors are $1 \text{ k}\Omega$ except for the variable resistor, which should be adjustable from 1 to $2 \text{ k}\Omega$.

flow is continuous (and in fact relatively smooth) in the space of x, \dot{x} , and \ddot{x} , since the discontinuity occurs only in the fourth derivative of x .

One might expect chaos in a system like Eq. (2) with the \dot{x}^2 term replaced with $|\dot{x}|$, but no such cases were found. However, there is a conservative case with three terms given by

$$\ddot{x} = -2\dot{x} \pm (|x| - 1), \quad (4)$$

albeit with very small Lyapunov exponents. The simplest dissipative chaotic flow with $\varphi(x) = |x|$ appears to be

$$\ddot{x} = -A\dot{x} - \dot{x} \pm (|x| - 1) \quad (5)$$

with a typical value of $A=0.6$. This case was described in detail by Linz and Sprott,¹³ and its behavior resembles the quadratic cases found here and elsewhere.⁴ It bears the same relation to the quadratic flows as the tent map does to the logistic map. Its attractor resembles the one found by Rössler.²

Equation (5) is well suited for solution using inverting operational amplifiers and diodes. The general strategy is to start with a voltage $-\ddot{x}$ and generate \ddot{x} , $-\dot{x}$, and x with successive inverting integrators. The weighted sum of the three signals and a constant term generated with a dc voltage source (a battery) are then fed back to the input of the first integrator as shown in Fig. 2. The circuit can be considered an oscillator with three 90° phase shifts and nonlinear positive feedback. If the resistors are 1Ω , the capacitors are 1 F , and the battery is 1 V , the circuit should work in real time and should produce chaotic oscillations when the variable resistor is adjusted to a value of $1/A \approx 1.67 \Omega$. However, the frequency at the first Hopf bifurcation at $A=1$ is only $1/2\pi$ Hz.

A more practical implementation uses resistors of $1 \text{ k}\Omega$ and capacitors of $0.1 \mu\text{F}$, giving a fundamental frequency of $f = 10^4/2\pi \approx 1592 \text{ Hz}$ at the first Hopf bifurcation. This frequency is well into the audio range so that the period doublings, periodic windows, and chaos are easily heard.¹⁴ The period doublings are even more pronounced when the signal x is integrated before amplification to enhance the low frequencies. Audio frequencies allow fast response to changes in control parameters, rapid accumulation of large data sets, easy display on an oscilloscope, and inexpensive digitization. The circuit has been constructed using inexpensive and non-critical components and could presumably be scaled to any

frequency from millihertz to megahertz and beyond. It has also been successfully simulated with the SPICE circuit simulator.¹⁵

One difficulty is that these circuits have a basin of attraction outside of which the dynamics are unbounded, which manifests itself in saturation of the op amps. If the op amps saturate, it is necessary to restart the circuit or otherwise bleed the charge off one or more of the capacitors. The op amps also need to have a relatively high slew rate. Otherwise, no difficulties were encountered in constructing any of the circuits. In particular, stray capacitance and inductance are not a problem at audio frequencies, and no parasitic oscillations were encountered.

The circuit in Fig. 2 provides three points of detailed comparison with theory—the frequency of oscillations, the values of A at which the various bifurcations occur, and the amplitude of the output voltage $x(t)$. All three agree with numerical calculations to within the precision of the electrical components (typically 10%) provided the forward voltage drop of the diodes (about 0.25 V for germanium) is taken into account by using $\varphi(x) = \max(|x| - 0.25, 0)$, which makes the bifurcations occur at a slightly lower value of A . Circuits that more accurately implement the $|x|$ operation with diodes are possible, but they generally require additional components, and their operation is less transparent. If the circuit were constructed with precision components ($\leq 1\%$), it should be possible to make a very detailed quantitative comparison of a chaotic experiment with theory. When the forward voltage drop of the diodes is taken into account, the circuit should permit automated bifurcation plots using a swept voltage source as the bifurcation parameter in place of the battery, which otherwise just determines the size of the attractor.

One simple way to digitize the signal is to feed it into the microphone or line input of a computer sound card. The signal can be displayed in oscilloscope fashion, or as a power spectrum or sonogram using the AUDIOSCOPE program.¹⁶ Alternately, one can capture the signal to a WAV file using the Windows Sound Recorder. If the sound is recorded in 8-bit mono, the file will consist of a short header followed by a string of bytes representing successive data samples. It is easy to write a program to extract and manipulate the data. Most sound cards can also record with 16-bit resolution, which is much more accurate, but it generates larger files, and it is more difficult to extract the data. Since sound cards usually have stereo input, it is possible to record simultaneously x and \dot{x} , for example, to produce phase-space plots, or $\dot{x}(t)$ can be numerically integrated. One problem is that the input to most sound cards is ac coupled, and so the very low-frequency information is lost, making it hard to produce bifurcation plots. It might be possible to bypass the input capacitors on the sound card and restore the dc level.

This circuit is similar in spirit to Chua's circuit,^{17,18} which uses two capacitors, an inductor, and diodes with operational amplifiers or transistors to provide a piecewise linear approximation to a cubic nonlinearity. Chua's circuit has a much more complicated jerk representation with many more than four terms, involving step functions, delta functions, and their products with derivatives of x . Because of the delta functions, the dynamics are not continuous in the space of (x, \dot{x}, \ddot{x}) . Since the contraction is not constant along the trajectory, it is more difficult to verify the Lyapunov exponents. Chua's circuit is more difficult to construct, scale to arbitrary frequencies, and analyze because of the inductor with its

frequency-dependent resistive losses, although a variant of Chua's circuit with only capacitors is possible.¹⁹ Three reactive components (capacitors or inductors) are required for chaos in systems with continuous flows so that the Kirchhoff representation of the circuit contains three first-order ODEs.

The realization of chaos in such a circuit raises the question of what is the simplest circuit using only operational amplifiers, resistors, capacitors, and diodes that exhibits chaos. The circuit in Fig. 2 with 18 components serves as a good starting point. It is not necessarily true that the simplest equations lead to the simplest circuits and vice versa, but they provide guidance for what circuits are worth exploration.

III. SINGLE-DIODE CASES

A simple variant of the circuit above uses a single diode. We need to distinguish between a forward diode for which $\varphi(x) = D(x) = \max(x, 0)$ and a reversed diode for which $\varphi(x) = R(x) = \min(x, 0)$. Note that $D(x) = (|x| + x)/2$ and $R(x) = (|x| - x)/2$, which implies that Eq. (5) can be solved in a circuit with a single diode. Such a circuit has the virtue that there is no dead zone (range of x over which neither diode conducts), although the attractor is displaced in x by the forward voltage drop of the diode. With such a circuit, the dc voltage source and resistor can be omitted. The simplest cases found with a single diode were

$$\ddot{x} = -0.3\ddot{x} - 0.3\dot{x} - D(x) + 1 \quad (6)$$

and

$$\ddot{x} = -0.3\ddot{x} - 0.3\dot{x} - R(x) - 1, \quad (7)$$

which have the same form as Eq. (5). Thus with an appropriate change in the values of two resistors in Fig. 2, the lower diode can be removed. Alternately, the polarity of the battery can be reversed and the upper diode removed, giving circuits with 17 components. In a practical circuit, it is sometimes necessary to reduce the battery voltage to avoid saturating the operational amplifiers or to increase it to improve the signal-to-noise ratio. The battery is usually replaced with the voltage source used to power the operational amplifiers, with the series resistor chosen appropriately to produce the desired input offset current. Some operational amplifiers have an offset adjustment that can be used in place of the voltage source and resistor. These single-diode examples are mathematically interesting because they are unique among those cases in Table I with the nonlinearity in the x term in that they have only a single fixed point and no localized extremum.

Since all the terms in Eq. (7) are negative, it might be possible to replace the second two active integrators with passive integrators (single RC circuits), thereby producing chaos in a circuit with a single operational amplifier. In an extensive numerical search for such solutions, none were found, presumably because the irreducible damping in the passive integrators is too severe. However, it is possible to construct a circuit with three operational amplifiers, a single diode, and one passive integrator as shown in Fig. 3 that solves Eq. (7). This circuit with 15 components has been constructed and tested. With passive integrators, one should be especially careful that the operational amplifiers don't saturate, since the signal levels at each may be rather different. Elwakil and Soliman²⁰ have also devised a chaotic circuit with 15 components using two operational amplifiers,

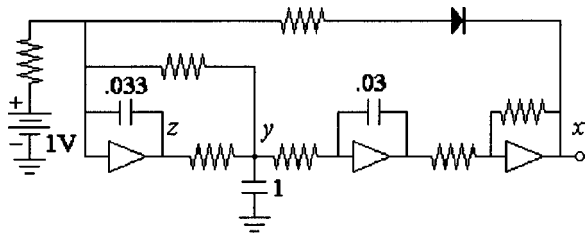


Fig. 3. Chaotic circuit implementation of Eq. (7) using three op amps. Capacitances are in microfarads, and all resistors are 1 kΩ. The resistor in series with the battery can be increased to prevent saturating the op amps.

three capacitors, two diodes, and eight resistors, but the equations required to model it are much more complicated.

Two other single-diode circuits with chaotic solutions have been developed and tested that use the noninverting input of one of the amplifiers. Both have only 12 components. Figure 4 shows one of these circuits that solves the equation

$$\ddot{x} = -0.25\ddot{x} - 0.25\dot{x} - R(x + 0.25\dot{x}) - 1, \quad (8)$$

which is very similar to Eq. (7). This circuit has been constructed, and its chaotic operation has been verified. Any of the components can be made adjustable to serve as a bifurcation parameter. The chaotic region is very narrow, a 5% change in the constant 0.25 will eliminate the chaos, but the forward voltage drop of the diode is not problematic. In this case, the battery voltage and series resistance cannot be increased arbitrarily since the inverting input is not a virtual ground.

IV. STEP FUNCTION CASES

Given that operational amplifiers are necessary for chaotic oscillations in circuits of this type, it is natural to consider using the inherent nonlinearity in the amplifier itself. Without feedback, a good operational amplifier acts as a comparator, abruptly switching output from a large positive to a large negative value as the input voltage crosses zero as shown in Fig. 1(f). In a real op amp, the switching speed is limited by the finite slew rate, and the saturation values are usually somewhat asymmetrical. The latter problem can be overcome by adjusting the positive and negative power supply voltages appropriately. This behavior suggests exploring systems in which the nonlinearity is $\text{sgn}(x)$, which is +1 for $x > 0$, -1 for $x < 0$, and 0 for $x = 0$. The simplest such cases found numerically were of the form

$$\ddot{x} = -0.5\ddot{x} - \dot{x} \pm [x - \text{sgn}(x)]. \quad (9)$$

This system has very different attractors for the plus and minus signs. With the plus sign, the attractor is a single-folded band similar to the Rössler attractor and the examples

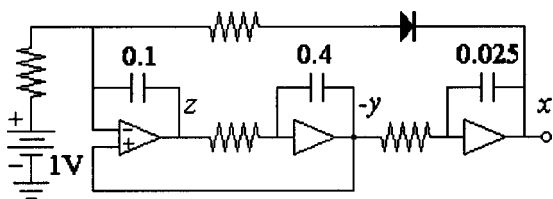


Fig. 4. Chaotic circuit implementation of Eq. (8) using three op amps. Capacitances are in microfarads, and all resistors are 1 kΩ.

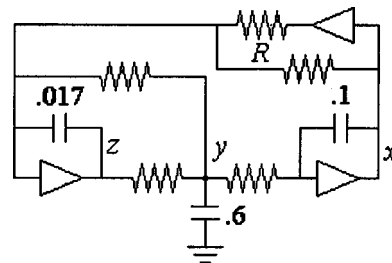


Fig. 5. Chaotic circuit implementation of Eq. (9) with the plus sign. Capacitances are in microfarads, and all resistors are 1 kΩ except for R , which should be adjusted to give a current of 1 mA when the upper op amp is saturated.

previously discussed. With the minus sign, a double-scroll attractor similar to the Lorenz attractor is possible.

With the plus sign, a particularly simple chaotic circuit is possible as shown in Fig. 5. This circuit has 11 components and is the simplest circuit of this class that was found. Although this circuit has been successfully tested, its operation is somewhat delicate because of its small basin of attraction. It exhibits hysteresis because of the finite gain-bandwidth product and slew rate of the operational amplifier. With the minus sign, an additional inverting amplifier is required in the feedback loop, but the operation is more stable and predictable. Because of the variety of attractors that can be obtained, this case offers a good opportunity for detailed comparison of theory with experiment. Figure 6 shows oscilloscope traces in the $x-\dot{x}$ plane of some of the attractors produced by a circuit that simulates the equation

$$\ddot{x} = -0.3\ddot{x} - \dot{x} - Bx + \text{sgn}(x) \quad (10)$$

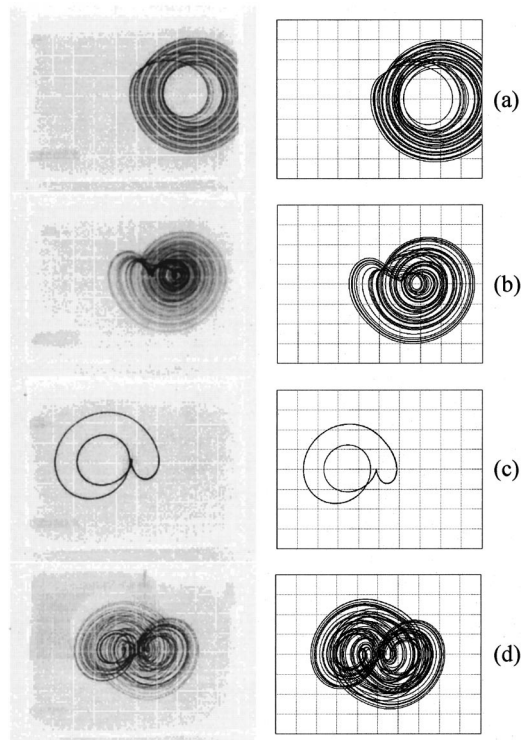


Fig. 6. Attractors produced by Eq. (10) in the $x-\dot{x}$ plane. In the left-hand column are oscilloscope traces for a circuit like Fig. 5 but with an extra inversion, and in the right-hand column are the corresponding numerical solutions on the same scale.

for various values of B along with the corresponding numerical prediction, plotted on the same scale.

The sgn function is closely related to the Heaviside function $H(x) = [\text{sgn}(x) + 1]/2$ (+1 for $x > 0$ and zero otherwise), which can be emulated electronically as shown in Fig. 1(g). The direction of the diode can be reversed to produce $-H(-x) = H(x) - 1$. Circuits based on this nonlinearity have been successfully tested, but they require two extra components (a diode and input resistor) and thus offer no particular advantage.

V. OTHER CASES

The operational amplifier comparator as shown in Fig. 1(f) is a limiting case of a more general function $\text{sgn}(x)\min(a|x|, b)$ in which a is the gain of the op amp and b is the saturation value. Typical operational amplifiers have open-loop gains of 10^4 – 10^6 . To test the sensitivity of the results to the quality of the comparator, cases were examined numerically in which the nonlinearity has the simple form $S(x) = \text{sgn}(x)\min(|x|, 1)$. This case corresponds to a unity-gain amplifier that saturates at an output of 1 V. Chaotic cases analogous to Eq. (9) were found, albeit with slightly different values of the coefficients:

$$\ddot{x} = -0.4\dot{x} - \dot{x} \pm [x - 2S(x)]. \quad (11)$$

The factor of 2 in front of $S(x)$ ensures that $x - 2S(x)$ is a nonmonotonic function of x , without which chaos is more difficult to achieve. Circuits based on this nonlinearity have been successfully tested, and their behavior mimics their sgn counterparts. A numerical search for circuits in which the chaos results from saturation of the op amp integrators did not reveal any such examples, although their existence cannot be excluded.

The function $S(x)$ can be considered a piecewise linear approximation to the hyperbolic tangent, $\tanh(x)$. Not surprisingly, chaos occurs in systems such as

$$\ddot{x} = -0.19\dot{x} - \dot{x} \pm [x - 2 \tanh(x)] \quad (12)$$

with behavior analogous to those cases above. A general feature of Eqs. (9)–(12) is an antisymmetric function of x with three zero crossings and a region of negative slope. Such functions naturally arise in cubic polynomials of the form $\pm(x - x^3)$ and lead to a number of chaotic examples as shown in Table I. A simple antisymmetric function with infinitely many zeros and regions of positive and negative slope is $\sin(x)$, for which a simple chaotic system is listed in Table I. The sine function can be approximated by an odd polynomial, $\sin(x) = x - x^3/6 + x^5/120 - \dots$. These last few systems are not ideal for electronic implementation, but they are listed for interest and completeness. Chaos has also been found in systems with $\varphi(x) = \cos(x)$, $\sinh(x)$, $\cosh(x)$, $\exp(x)$, $\exp(-|x|)$, and $\exp(-x^2)$.

Systems involving delta functions (derivatives of the Heaviside function) also lead to chaotic solutions as Chua's circuit attests. Such systems can be studied numerically by imposing a jump condition where the trajectory crosses the singularity. Another interesting class is hysteretic functions in which $\varphi(x)$ is multivalued. Since the flow is discontinuous for delta functions and hysteretic functions, chaos is possible with less than three variables. A two-dimensional chaotic circuit with 13 components based on this idea has been developed by Tamaševičius *et al.*²¹

VI. DISCUSSION

Most of the dissipative chaotic systems found in this study are of the general form

$$\ddot{x} + A\dot{x} + \dot{x} = G(x). \quad (13)$$

Integrating each term reveals that this system is a damped harmonic oscillator driven by a nonlinear memory term that involves the integral of $G(x)$. Such an equation often arises in the feedback control of an oscillator in which the experimentally accessible variable is a transformed and integrated version of the fundamental dynamical variable. Despite its importance and the richness of its dynamics, this system, with a nonlinear $G(x)$, seems to have been studied relatively little. Coulett, Tresser, and Arneodo observed chaos in numerical simulations with a cubic²² and a special piecewise linear^{23,24} form of $G(x)$, and Rul'kov *et al.*^{25,26} devised an RLC circuit with an unspecified nonlinear amplifier to produce chaos with a particular form of $G(x)$.

Many forms of $G(x)$ lead to chaos. For bounded solutions, $G(x)$ must average to zero along the orbit,¹³ which means that any continuous $G(x)$ must have at least one zero at $x = x^*$. The stability of the fixed point at $(x^*, 0, 0)$ is determined by the solutions of the eigenvalue equation $\lambda^3 + A\lambda^2 + \lambda - G' = 0$, where $G' = dG/dx$ evaluated at $x = x^*$. This point is locally stable for $-A \leq G' \leq 0$ and undergoes a Hopf bifurcation at $G' = -A$, where $\lambda = \pm i$. Thus one would expect chaotic systems of this form to require a nonlinearity with either a positive slope at its zero crossing or a sizable negative slope, implying a negative resistance in the corresponding circuit model. Systems with $G' > 0$ apparently require at least two fixed points for chaos, but systems with $G' < -A$ only need one. All the cases studied have these features. Chua and Ayrom²⁷ describe saturating op-amp circuits with a variety of piecewise linear characteristics.

It is interesting to ask for what function $G(x)$ the system in Eq. (13) is most chaotic. Of the cases studied, the largest Lyapunov exponents occur for systems of the form

$$\ddot{x} + A\dot{x} + \dot{x} = B[x - \text{sgn}(x)]. \quad (14)$$

Using a variant of simulated annealing,²⁸ the parameters A and B were adjusted to maximize the Lyapunov exponent. The result was $A = 0.55$ and $B = 2.84$, for which the Lyapunov exponents (base e) are $(1.055, 0, -1.655)$, giving an attractor with a Kaplan–Yorke dimension²⁹ of $D_{KY} = 2.637$. The attractor is contained within a thin torus that nearly touches the boundary of its small basin of attraction so that initial conditions must be chosen carefully to produce bounded solutions. The trajectory is repeatedly thrown back and forth between the vicinity of the unstable fixed points at $x^* = \pm 1$.

It is also interesting to determine the least nonlinear form of $G(x)$ for which chaos occurs in Eq. (13), which we take to mean the two-part piecewise linear function with the smallest bend at the knee. Without loss of generality, we can take $G(x) = -\min(Bx, Cx + B - C)$, which is scaled so that the unstable fixed point is at $x = 0$ and the knee is at $x = 1$. We minimize the angle at the bend, $\theta = |\tan^{-1}(B) - \tan^{-1}(C)|$, by the same method as above and conclude that the minimum θ occurs for $B \approx -C$, which is equivalent to the case with $G(x) = B|x| - 1$. For $A = 0$ (the conservative case), chaos was found for values of B as small as 0.01 ($\theta \approx 1.15^\circ$) over

a very limited range of initial conditions with a very small Lyapunov exponent (~ 0.001). For $A > 0$ (the dissipative case), the smallest B for which chaos was found had $A = 0.025$ and $B = 0.468$ ($\theta \approx 50.2^\circ$). The basin of attraction is very small, and the chaotic attractor coexists with a nearby limit cycle.

Systems of the form of Eq. (13) are ripe for numerical, analytical, and electrical exploration and offer exceptional projects for students. They may also have practical application in secure communications and broadband signal generation.

ACKNOWLEDGMENTS

I am grateful to Stefan Linz, Lucas Finco, and Tom Lovell for useful discussions.

^{a)}Electronic mail: sprott@juno.physics.wisc.edu

¹E. N. Lorenz, "Deterministic nonperiodic flow," *J. Atmos. Sci.* **20**, 130–141 (1963).
²O. E. Rössler, "An equation for continuous chaos," *Phys. Lett. A* **57**, 397–398 (1976).
³O. E. Rössler, "Continuous chaos—Four prototype equations," *Ann. (N.Y.) Acad. Sci.* **316**, 376–392 (1979).
⁴J. C. Sprott, "Some simple chaotic flows," *Phys. Rev. E* **50**, R647–R650 (1994).
⁵H. P. W. Gottlieb, "Question #38. What is the simplest jerk function that gives chaos?" *Am. J. Phys.* **64**, 525 (1996).
⁶S. J. Linz, "Nonlinear dynamical models and jerky motion," *Am. J. Phys.* **65**, 523–526 (1997).
⁷J. C. Sprott, "Some simple chaotic jerk functions," *Am. J. Phys.* **65**, 537–543 (1997).
⁸J. C. Sprott, "Simplest dissipative chaotic flow," *Phys. Lett. A* **228**, 271–274 (1997).
⁹R. Eichhorn, S. J. Linz, and P. Hänggi, "Transformations of nonlinear dynamical systems to jerky motion and its application to minimal chaotic flows," *Phys. Rev. E* **58**, 7151–7164 (1998).
¹⁰Zhang Fu and J. Heidel, "Non-chaotic behaviour in three-dimensional quadratic systems," *Nonlinearity* **10**, 1289–1303 (1997).
¹¹J. Heidel and Zhang Fu, "Nonchaotic behaviour in three-dimensional quadratic systems. II. The conservative case," *Nonlinearity* **12**, 617–633 (1999).
¹²A. Wolf, J. B. Swift, H. L. Swinney, and J. A. Vastano, "Determining Lyapunov exponents from a time series," *Physica D* **16**, 285–317 (1985).

¹³S. J. Linz and J. C. Sprott, "Elementary chaotic flow," *Phys. Lett. A* **259**, 240–245 (1999).
¹⁴More detail about the system in Eq. (5), including a sound file of the bifurcations as $1/A$ is increased can be found at <http://sprott.physics.wisc.edu/chaos/abschaos.htm>.
¹⁵TOPSPICE, a PC version of the SPICE circuit simulator is available from Penzar Development. A demo version can be found at <http://www.penzar.com/topspice.htm>.
¹⁶G. Marlow, *Audioscope* (Physics Academic Software, Raleigh, NC, 1999).
¹⁷T. Matsumoto, L. O. Chua, and M. Komoro, "The double scroll," *IEEE Trans. Circuits Syst.* **CAS-32**, 797–818 (1985).
¹⁸T. Matsumoto, L. O. Chua, and M. Komoro, "Birth and death of the double scroll," *Physica D* **24**, 97–124 (1987).
¹⁹Ö. Morgül, "Inductorless realisation of chua oscillator," *Electron. Lett.* **31**, 1303–1304 (1995).
²⁰A. S. Elwakil and A. M. Soliman, "Two modified for chaos negative impedance converter op amp oscillators with symmetrical and antisymmetrical nonlinearities," *Int. J. Bifurcation Chaos Appl. Sci. Eng.* **8**, 1335–1346 (1998).
²¹A. Tamaševičius, G. Mykolaitis, and A. Namažūnas, "Double scroll in a simple '2D' chaotic oscillator," *Electron. Lett.* **32**, 1250–1251 (1996).
²²P. Coulet, C. Tresser, and A. Arnéodo, "Transition to stochasticity for a class of forced oscillators," *Phys. Lett. A* **72**, 268–270 (1979).
²³A. Arneodo, P. Coulet, and C. Tresser, "Possible new strange attractors with spiral structure," *Commun. Math. Phys.* **79**, 573–579 (1981).
²⁴A. Arneodo, P. Coulet, and C. Tresser, "Oscillators with chaotic behavior: An illustration of a theorem by Shil'nikov," *J. Stat. Phys.* **27**, 171–182 (1982).
²⁵N. F. Rul'kov, A. R. Volkovskii, A. Rodríguez-Lozano, E. Del Río, and M. G. Velarde, "Mutual synchronization of chaotic self-oscillators with dissipative coupling," *Int. J. Bifurcation Chaos Appl. Sci. Eng.* **2**, 669–676 (1992).
²⁶E. Del Río, M. G. Velarde, A. Rodríguez-Lozano, N. F. Rul'kov, and A. R. Volkovskii, "Experimental evidence for synchronous behavior of chaotic nonlinear oscillators with unidirectional or mutual driving," *Int. J. Bifurcation Chaos Appl. Sci. Eng.* **4**, 1003–1009 (1994).
²⁷L. O. Chua and F. Ayrom, "Designing non-linear single op-amp circuits: A cookbook approach," *Int. J. Circuit Theory Appl.* **13**, 235–268 (1985).
²⁸W. H. Press, S. A. Teukolsky, W. T. Vetterling, and B. P. Flannery, *Numerical Recipes in C: The Art of Scientific Computing* (Cambridge U.P., Cambridge, 1993), p. 436 (also available on-line at http://www.ulib.org/webRoot/Books/Numerical_Recipes/).
²⁹J. Kaplan and J. Yorke, in *Functional Differential Equations and the Approximation of Fixed Points*, edited by H. O. Peitgen and H. O. Walther [*Lect. Notes Math.* **730**, 204 (1979)].